

# Numerical Simulation of End Plug Resistance Welding Process in Nuclear Fuel Rods

Tae-Hyung Na<sup>ab\*</sup>, Bo-Hee Lee<sup>a</sup>, Se-Ik Son<sup>a</sup>

<sup>a</sup> PWR Process Engineering team, KEPCO Nuclear fuel, Daejeon Republic of Korea

<sup>b</sup> Central Research Institute, Korea Hydro & Nuclear Power Co., Ltd, Daejeon, Republic Korea

\*Corresponding author: taehyung.na@khnp.co.kr

## 1. Introduction

Nuclear fuel rods are designed to prevent damage to cladding materials during combustion in a reactor as well as to serve as a pressure vessel preventing any leakage of radioactive fission material. For reliable performance of fuel assemblies, a high level of weld integrity of nuclear fuel rod end plugs is crucial. In a recent study by Park et al. [1], weld quality was evaluated through a burst test to assess the quality of fuel rods. Na et al. [2] were the first to conduct a quality monitoring study to confirm the end plug weldment integrity of a nuclear fuel rod using current, dynamic resistance, and welding force.

During resistance upset butt welding, deformation, stress, and strain are generated in the workpieces. These mechanical features strongly influence the properties of the weld joint. Therefore, it is very important to understand the temperature changes, deformation, and phase transformation of the metallographic structure during the welding process. A single-phase AC (Alternative Current) welder is used for the resistance butt welding of a nuclear fuel rod. The welding time is 1 cycle (1/60 second, 16.67 milliseconds) and very short and high current is used. The finite element numerical modeling and simulation provide a valuable way of studying the spot welding process. The purpose of this study is to clarify the mechanism of end plug welding process in nuclear fuel rod.

## 2. Welding Method and Material for Simulation

### 2.1 Welding Method

In this study, resistance upset butt welding is employed for welding the fuel rod end plug. Fig. 1 shows the schematic illustration of the welding process. As shown in Fig. 1, a high current is applied for a short time (1 cycle) while the fuel rod and tube are in contact with each other by using the force of a pneumatic cylinder. The end plug (EP) and the cladding tube (CT) are joined by the resistance heat generated at this time.

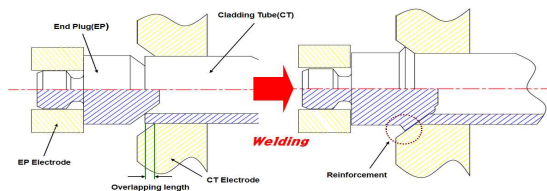


Fig. 1 Weld method diagram of cladding tube and end plug

The resistance welding machine in this study uses a single phase alternative current power source. The major welding variables in the resistance welding of these fuel rods are current, overlapping length and force. The amount of protruding tube based on the end part of the CT electrode is called the overlapping length. The overlapping length and the end plug are welded together, and the displacement of the EP electrode during 1 cycle indicates the change of the overlapping length. The cladding tube was 9.5 mm in diameter and 0.6 mm in thickness.

### 2.2 Materials for Simulation

For nuclear fuel rod, zirconium alloy is commonly used. As Zircaloy-4/ZIRLO could have tendency to produce hydrides, the content of Ni which causes embrittlement of the cladding was reduced while Fe was added to decrease in the absorption rate of hydrogen leading to well-maintained corrosion resistance. Due to these characteristics, these two alloys are currently the most used materials. The chemical compositions of Zircaloy-4/ZIRLO are shown in Table 1.

Table 1 Chemical composition of zirconium alloys [3]

Element	Zircaloy-4	ZIRLO
Sn	1.20-1.45	0.90-1.30
Fe	0.18-0.24	0.80-1.40
Cr	0.07-0.13	-
Ni	<0.007	-
Fe+Cr	0.28-0.37	-
Nb	-	0.80-1.40
Oxygen	0.10-0.15	0.10-0.16
Zr	Balance	Balance

The mechanical properties of Zircaloy-4 and ZIRLO are listed in Table 2. The manufacturing process was optimized to obtain nearly the same mechanical properties for both Zircaloy-4 and ZIRLO. Therefore, even though there are minor differences between these materials, the mechanical properties are considered identical.

Table 2 Mechanical properties of zirconium alloys [3]

Property	Zircaloy-4	ZIRLO
YS (MPa)	613.88	596.8
TS (MPa)	819.04	794.35
EL (%)	14.67	15.5

### 3. Simulation for Tube-End Plug Resistance Welding

In order to understand the phenomenon occurring during the welding of the fuel rod end plug, simulation was conducted to identify the welding mechanism. As described by Nielsen et al. [4, 5], resistance welding is generally influenced by thermal, electrical, and mechanical factors. Thus, the simulation is performed by coupling these three factors. Fig. 2 presents the results of modeling the end plug and tube for the simulation and generating the finite elements. As shown in the figure, the axisymmetric model was formed so as to correspond with the welding conditions, and it was simulated by rotating it by 90 degrees for convenience. In the figure, 1 and 3 denote the cladding tube (CT) and end plug (EP), 2 is the CT electrode, and 4 is the EP electrode. The materials and mechanical properties of CT and EP are shown in Tables 1 and 2. The finite elements were densely formed around the joint to obtain the best simulation results.

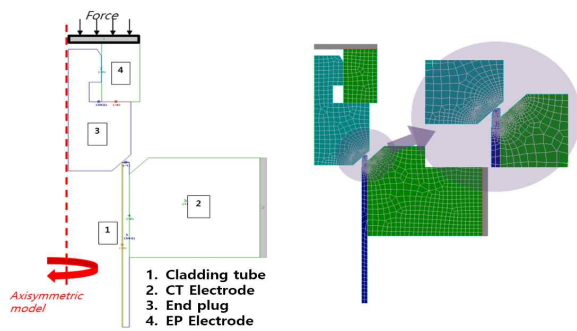


Fig. 2 Geometry and generated finite elements for simulation

In resistance welding, current is very important. In particular, the performance of the welding machine depends on the conduction angle of the welding power source. In this study, the current formed during welding is measured and accurate welding simulation results are derived by modeling, as shown in Fig. 3, based on the measured current pattern.

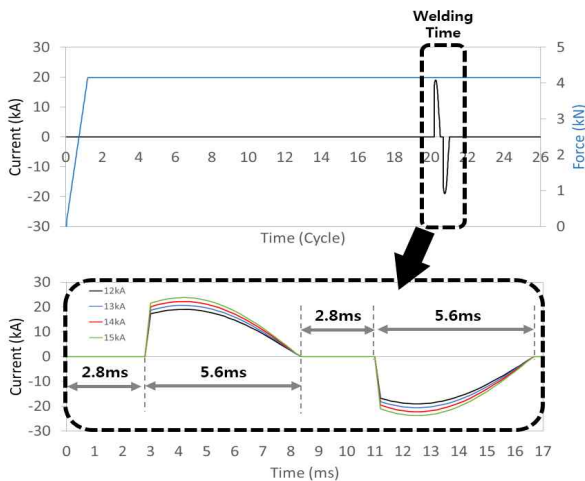


Fig. 3 Simulation (current)

### 4. Simulation Results

The following simulations were carried out to identify the mechanism of resistance welding of the fuel rod and to analyze the welding phenomena. [Welding Parameter: Current(14kA), Welding Force(4,300N), Overlapping length(0.8mm)]. Simulation shows the welding time for 1 cycle. As shown in Fig. 4, the simulation results are divided into five sections, A to E, and are verified in each section. Each section is defined as follows; 1st half cycle: current start point (A) / current peak point (B) / cooling time point (C), 2nd half cycle: current peak point (D) / current fall point (E).

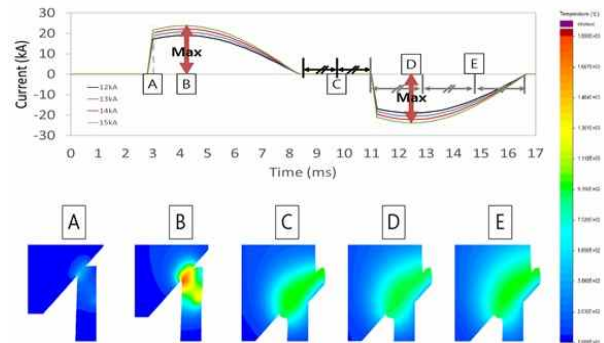


Fig. 4 Welding simulation images by each section

Fig. 4 also shows the results obtained from each major point (A to E) through the numerical simulation. A is the point where the initial current begins to flow. The end plug and the tube are initially contacted by applying force. In general, the resistance during welding is expressed by the sum of the bulk resistance and the contact resistance of the material. In the initial stage, the contact cross-sectional area between the end plug and the tube is small. As a result, the total resistance is very large. When the current begins to flow through the power supply, the temperature rises and the bulk resistance increases, but the contact area increases as the electrode displacement is formed, and the contact resistance sharply decreases. That is, the total resistance becomes lowered. B is the point at which the peak current flows in the 1st half cycle, and the welding temperature increases sharply. As the current increases, the amount of heat generated increases resulting in larger amount of melted material. In the B-C section, heated metal flow is generated in the inner and outer direction by the applied force, and most of the weldment and reinforcement is formed as the cross-sectional contact area is widened. After the peak current of the 1st half cycle, the current is decreased, but the movement of the electrode is maintained by the generated melting. D is the point where the peak current of the 2nd half cycle and the junction cross-section of the weldment is already very wide, and thus bulk resistance mainly occurs rather than contact resistance. Therefore, even if current flows, sufficient heating to generate melting is not attained and the temperature does not rise because

of low total resistance. E is the point at which the current of the 2nd half cycle decreases, and the temperature and resistance of the weld remain almost unchanged.

## **5. Conclusions**

From the experiment and simulation for the end plug resistance welding of PWR nuclear fuel rods, the main results obtained from this study are as given below.

(1) Analysis of weld mechanism for process of resistance welding of the fuel rod end plug revealed that the heat generated in the weld at the beginning of welding is caused by the contact resistance at the part where the end plug and the cladding tube are in contact.

(2) Due to low heat generation during the 2nd half cycle, the effect of the 2nd half cycle on weldment is negligible.

(3) Most welding and plastic deformation occurred during the 1st half cycle.

Therefore, Nuclear fuel rod resistance welding is mostly determined during the 1<sup>st</sup> half cycle. Based on the welding analysis performed in this study, simulation will be conducted and analyzed by changing the weld parameters in terms of excessive heat input and insufficient conditions in the future.

## **REFERENCES**

- [1] J.Y Park, T.H Na, T.H Lee, J.H Lee, B.Y , J.S Kim, Effect of applied current on the formation of defect in PWR nuclear fuel rods in resistance pressure welding process, Journal of Nuclear Science and Technology Vol.52, pp.748-757, 2015.
- [2] T.H Na, S.J Na, M.H Ko, D.S Hwang, Algorithm development for quality monitoring on end plug resistance weldment of nuclear fuel rods. The International Journal of Advanced Manufacturing Technology, Vol.85, pp.991-1006, 2016.
- [3] T.H Na, B.H Lee, M.W Kim, S.J Na, Quality monitoring of end plug resistance weldment for nuclear fuel rods by electrode displacement, The International Journal of Advanced Manufacturing Technology, 2018 DOI : 10.1007/s00170-018-2642-1
- [4] C.V Nielsen, W Zhang, L.M Alves, N Bay , P.A.F Martins, Modeling of Thermo-Electro-Mechanical Manufacturing Processes with Applications in Metal Forming and Resistance Welding. Springer Science & Business Media, 2012.
- [5] C.V Nielsen, W Zhang, P.A.F Martins, N Bay, 3D numerical simulation of projection welding of square nuts to sheets. Journal of Material Processing Technology Vol.215 pp.171-180, 2015.